Technical University of Denmark

DTU

Fatigue damage propagation in unidirectional glass fibre reinforced composites

Hansen, Jens Zangenberg; Alzamora Guzman, Vladimir Joel; Østergaard, R.C.; Brøndsted, Povl

Link back to DTU Orbit

DTU Library
Technical Information Center of Denmark

FATIGUE DAMAGE PROPAGATION IN UNIDIRECTIONAL GLASS FIBRE REINFORCED COMPOSITES

J. Zangenberg[1,2*], V. J. A. Guzman[2], R. C. Østergaard[1], P. Brøndsted[2]

[1]*LM Wind Power, Composite Mechanics, Jupitervej 6, 6000 Kolding, Denmark*
[2]*Department of Wind Energy, Section of Composites and Materials Mechanics, Technical University of Denmark, Risø Campus, Frederiksborgvej 399, DK-4000 Roskilde, Denmark*
* *jzan@dtu.dk, jezh@lmwindpower.com*

Keywords: Fatigue damage, stiffness degradation, fibre breaks

Abstract
Damage progression in unidirectional glass fibre reinforced composites exposed to tension fatigue is investigated, and a quantitative explanation is given for the observed stiffness loss. The stiffness degradation during fatigue is directly related to fibre breaks in the load-carrying axial fibre bundles. The underlying mechanisms are examined using digital microscopy, and it is postulated that fatigue damage initiates due to stress concentrations between the backing (transverse) layer and the unidirectional layer, followed by a cyclic fretting and axial fibre debonding. This fretting mechanism needs further attention and understanding in order to improve the fatigue life-time of glass fibre reinforced composites.

1 Introduction

Stiffness degradation of unidirectional Glass Fibre Reinforced Polymers (GFRP's) under tension fatigue loading is a well-known phenomenon [1], [2], [3]. Nonetheless, there has not been any unambiguous explanation for what causes this damage or stiffness loss. Simple calculations show that the stiffness loss of the composite cannot be solely explained by matrix cracks alone, which is why axial load-carrying fibre breaks must occur. This fact has been reported by different researchers e.g. Gamstedt & Talreja [4]. For cross-ply (or angle-ply) laminates the observed fatigue damage can be related directly to cracking in the transverse plies, and these phenomenon have been well described both for static and cyclic loading [5], [6], [7], [8], [9]. A typical fatigue process for a unidirectional GFRP under constant stress is illustrated in Fig. 1(a) showing two different common types of observable damage: stiffness degradation and damping increase. The phases in Fig. 1(b) are characterised by a non-linear initiation stage (phase I) lasting approximately 10-15% of the lifetime, a stage of uniform damage propagation (phase II) lasting approximately 70-80% of the life-time, and finally phase III where damage is localised and leads to final failure [1]. The magnitude of the stiffness loss is dependent on loading type, layup sequence, and material properties [9], [3]. Monitoring stiffness loss (or damping) can therefore be used to determine the damage level in a GFRP [10]. For a unidirectional GFRP there does not seem to be a definitive conclusion for the reason of fatigue damage, and the present study is a quantitative analysis of the fatigue damage mechanisms that govern the life-time of a GFRP. The experimental observations are analysed using microscopy, and a damage sequence in relation to tension fatigue is postulated.
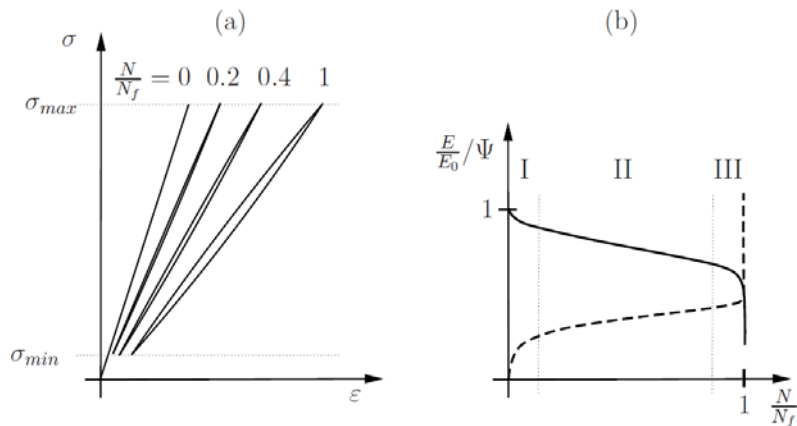
Figure 1. Sketch of a typical fatigue process observed in a glass fibre reinforced composite. (a) Stress/strain relation for a stress controlled fatigue test showing evolution of damage as function of normalised number of cycles. (b) Stiffness degradation (-) and damping propagation (--).

2 Materials and method

Standard stress-controlled tension-tension fatigue experiments (f = 5Hz, $R = \sigma_{min}/\sigma_{max} = 0.1$, $\varepsilon_{max} = 0.8\%$) are conducted on a number of 4-layered GFRP's with different fibre volume contents. End tabs are mounted on the specimens and loaded in the axial direction using a servo-hydraulic Instron test machine. The axial strain is measured using two extensometers placed back-to-back. The material system is a high-performance glass fibre fabric and a thermoset polyester, manufactured using the VARTM process. The two sides of the fabric are illustrated in Fig. 2. The stitching (polyester thread) is visible on one side, and the backing on the other. Backing fibres are only used to keep and support the fabric in place while handling/layup. The thickness of the backing layer is approximately 10% of the axial bundles/tows.
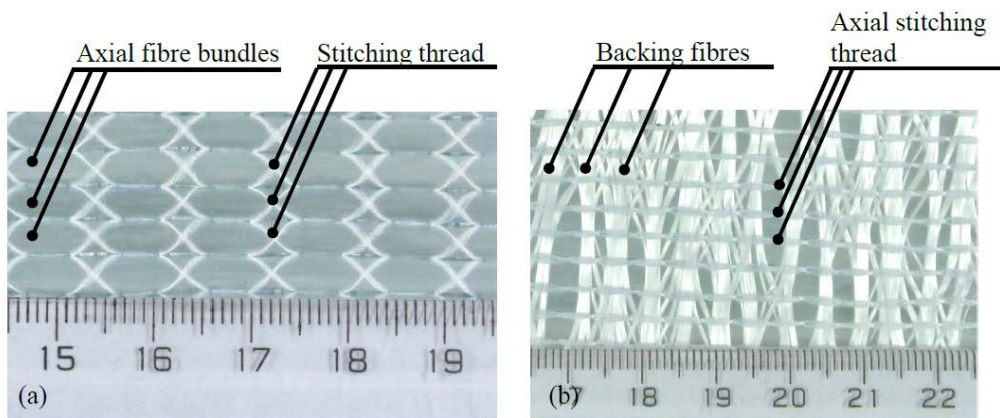

Figure 2. Illustration of fabric. (a) Top side of fabric. Axial bundles and double equal pillar tricot stitching. (b) Bottom (backing) side of fabric. Axial bundles are placed underneath the backing in horizontal direction.

At first, stiffness degradation curves, similar to Fig. 1(b), are established for each fibre volume fraction (FVF) to gain information about the life-time and the stiffness-loss of the composite. Phase II of the stiffness degradation curve is assumed to follow a linear dependency meaning that the degradation rate, a, can be expressed as, [1]:

$$a = \frac{d(-E/E_0)}{dN},$$ (1)

where E_0 and E are the initial and degraded stiffness modulus after N cycles, respectively. Eq. (1) will be used to determine the rate of change for the different FVF's considered. Secondly, fatigue experiments are terminated prior to final failure somewhere in phase II, see Fig. 1(b), to obtain a certain amount of damage in the materials. Thereupon, the interior damage is considered using polarised microscopy, and the resin is afterwards burned away in an oven in order to inspect for broken fibres in the axial bundles. Microscopic inspection using a DeltaPix microscope and digital image processing in MATLAB are used to evaluate the number of broken axial fibres. Finally, the underlying mechanisms that cause the material damage during the fatigue experiments are analysed, and a damage scheme is presented.

3 Results

3.1 Cycles to failure and stiffness degradation rate

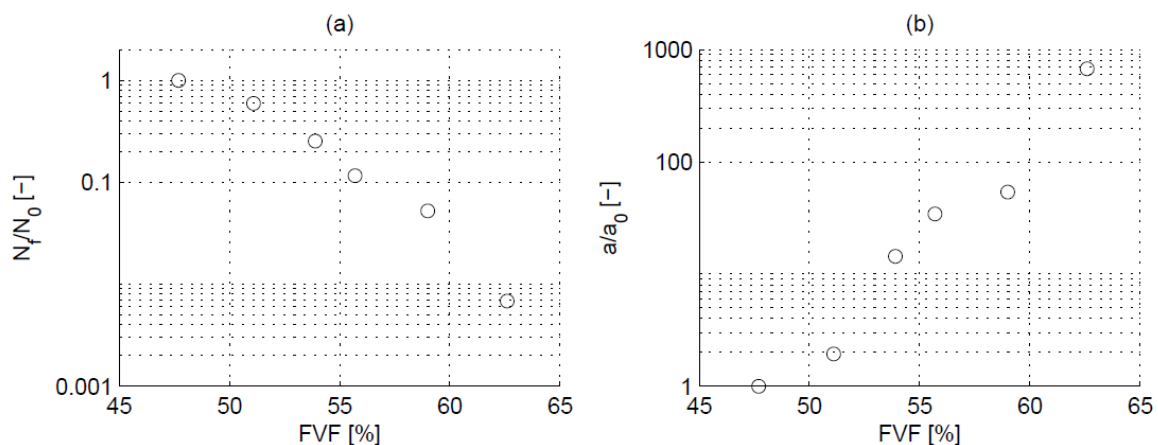The normalised number of cycles to failure, and the normalised stiffness degradation rate is presented in Fig. 3.

Figure 3. Result of fatigue experiments of GFRP's with different FVF's. Each circle presents the mean value of at least three experiments, and the results are normalised with the value from the experiment with the lowest FVF. (a) Number of cycles to failure. (b) Stiffness degradation rate, Eq. (1).

It is observed that there is a strong influence of the FVF on the fatigue life-time and the damage propagation rate.

3.2 Stiffness degradation mechanisms in phase II

In order to detect the stiffness degradation mechanisms in phase II, see Fig. 1(b), the fatigue damaged specimens are analysed. Prior to burning the resin, polarised microscopy is used to inspect for changes in the strain field within the interior of the specimen. A typical micrograph showing the interior fatigue damage is presented in Fig. 4. There is a considerable amount of damage due to fatigue, and a closer examination reveals that the damage is concentrated in regions where the backing fibres are crossing each other, see magnification in Fig. 4. From the magnification in Fig. 4, it is also observed that there is a kind of delamination (transverse cracks) in the direction along the backing fibres. Beneath the crossing points of the backing, an extensive amount of fibre debonding is observed in the axial load-carrying fibre bundles, which is shown in Fig. 5. Matrix cracks are apparently not present within the samples. The observations in Fig. 4 and 5 are found in all specimens independent of the FVF.
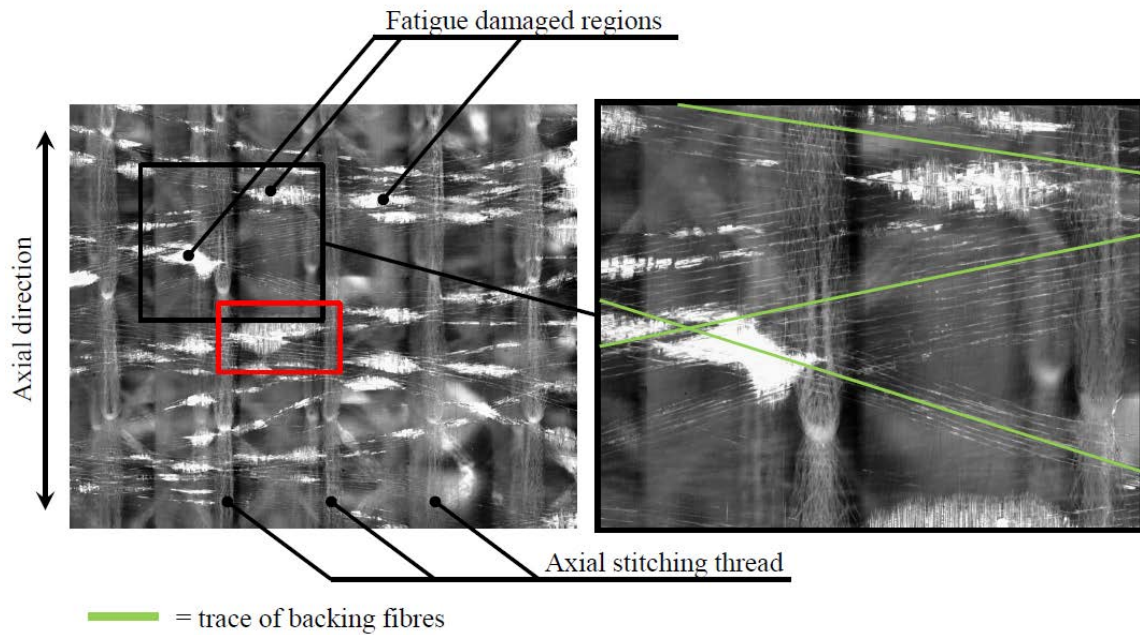
Figure 4. Fatigue damage in a unidirectional GFRP. The red box is magnified in Fig. 5.
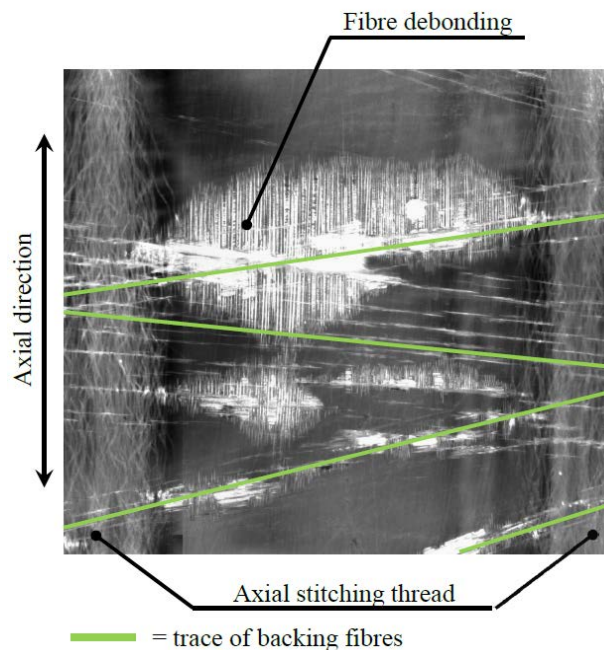
Figure 5. Magnification of the red box in Fig. 4 showing fibre debonding in the axial fibres beneath the backing layer.

The resin is burned away, and potentially broken fibres are investigated in the axial bundles in the regions of contact to the backing fibres. A typical specimen after burning the resin is shown in Fig. 6. Note that the stitching thread is also removed during the burning process since it is made of polyester. From Fig. 6(b) it is evident that the method of burning the resin can also be used to estimate the in-plane waviness of the axial bundles. However, this is outside the scope of the present study and has been left out.

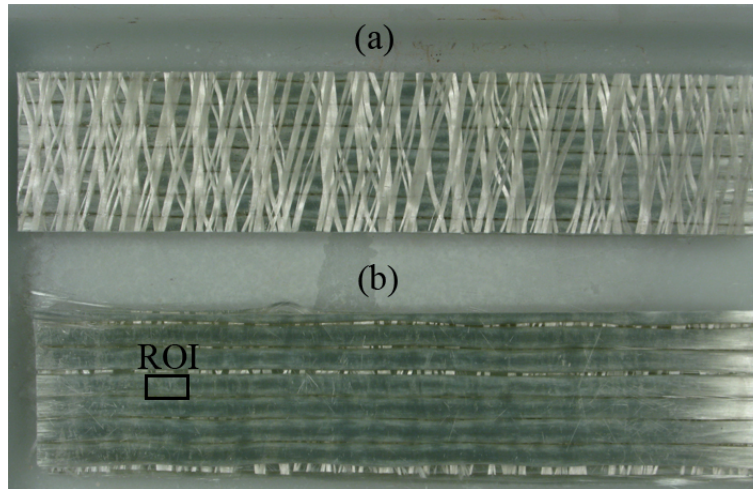**Figure 6.** Specimen after removal of the resin. Axial fibre direction is horizontal. (a) With backing fibres. (b) Without backing fibres. ROI = Region Of Interest.

Upon microscopic inspection in the region of interest, Fig. 6(b), it is found that there is a severe concentration of broken axial fibres underneath the backing and the stitching thread. A typical image is presented in Fig. 7 where a severe concentration of broken fibres is found beneath the backing (only backing side is shown with backing fibres removed).

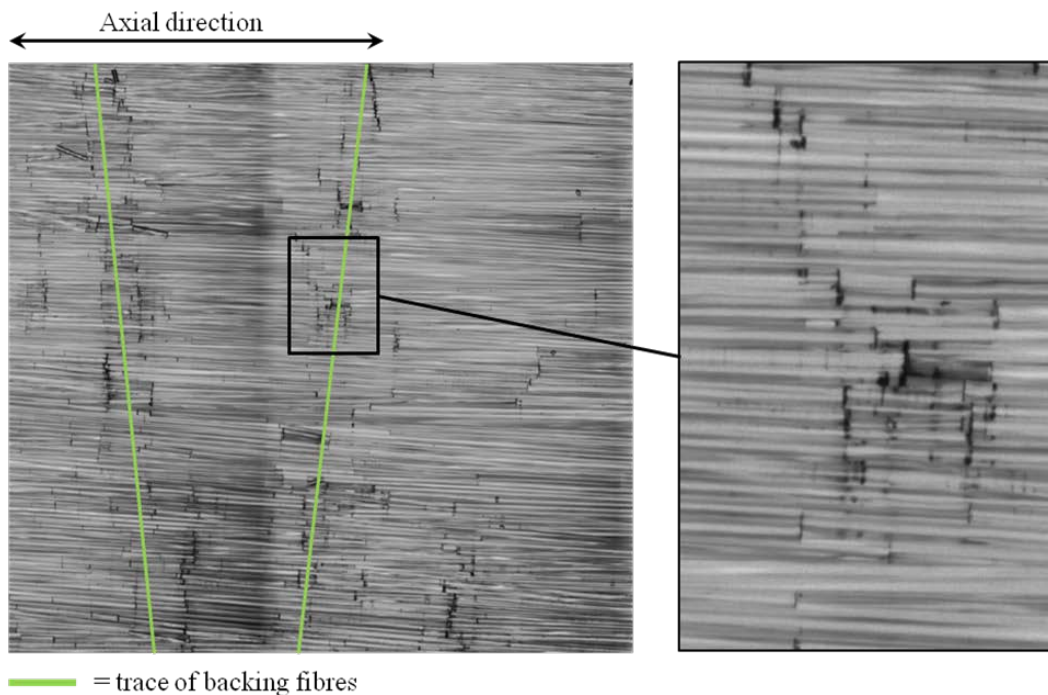**Figure 7.** Micrograph of broken fibres underneath the backing for the region shown in Fig. 6. Note the extensive amount of fibre breaks beneath the location of the backing layer.

The broken axial fibres are observed in all specimens independent of the FVF. Ongoing work will characterise the amount of broken fibres found in the axial bundles, and relate it to the different regions of fatigue damage.

4 Discussion

4.1 Cycles to failure and stiffness degradation rate

From Fig. 3(a) it is evident that the fatigue life is highly dependent on the composite microstructure reflected in terms of the FVF. Furthermore, the stiffness degradation rate, Fig. 3(b), is substantially larger for increasing FVF meaning that fatigue damage propagates faster for larger FVF's. It is recalled that all experiments are carried out for the same maximum initial strain level, which means that the specimens with the larger FVF experience a larger stress due to the increased stiffness. However, this increase in stress cannot explain the lower fatigue lifetime. For the present range of FVF's, there does not seem to be a plateau for an optimum fatigue performance. However, there seem to be a power law dependency on both the number of cycles to failure, Fig. 3(a), and the stiffness degradation rate, Fig. 3(b), as a function of the FVF. Even though the stiffness degradation rates are different for each FVF, the overall shape of the curves is similar (not shown, comparable to Fig. 1(b)). This indicates that the damage process is identical for all samples, but the magnitude of the propagation is different. In a given application it is essential to be aware of the material behaviour reported in Fig. 3 since local variations in the FVF within the material can cause different resistance to fatigue.

4.2 Stiffness degradation mechanisms in phase II

The fatigue damage process has been investigated in phase II, and it is shown that damage initiates underneath the backing or crossing points of the stitching thread. The observed damage behaviour is consistent for all FVF's considered, which indicates that similar damage processes occur but with different rate, cf. Fig. 3(b).

4.3 Fatigue damage process in GFRP

Distinguishing between the different fatigue damage phases presented in Fig. 1(b), an explanation of the mechanisms of tensile fatigue damage failure in an axially loaded unidirectional GFRP is given in the following. It is noted that this scheme is only valid for material systems containing some kind of fibre backing arrangement, and not for wound plates without backing. Here, the fatigue life is improved and only governed by differences in the fibre architecture (touching fibres, local clustering, waviness, etc.) and the properties of the constituents (fibre, matrix, and interface). Obviously, these mechanisms are also active in the present, but they are not the detrimental cause of fatigue failure.

Phase I: The duration of phase I is approximately 10-15% of the entire fatigue life-time, and typical observed stiffness loss is within a few percent. Damage is characterised by (transverse) cracking/failure of the backing layer causing delamination within the backing layer and along the interface to the axial fibres. Shear and interlaminar properties are believed to be essential for this phase. Release of internal residual stress due to curing is also an important issue that needs further investigation for this phase.

Phase II: Lasting most of the life-time with a somewhat constant stiffness degradation rate, damage consists of sliding friction (fretting, rubbing) between the backing layer (as well as the stitching thread) and the axial fibres. As the cyclic load is applied, the fretting causes fibre breaks in the axial fibres. Due to the stress transfer at the broken fibre ends in the load-carrying bundles, fibre debonding occurs and propagates along the axial direction. Fibre fracture and debonding continues throughout the phase and cause both a loss of stiffness and an increase in material damping. Interfacial fibre/matrix properties are considered crucial.

Phase III: Near the last 5-10% of the life-time of the GFRP, damage progression of phase 2 is localised and leads to final failure. Final failure can be observed near the end tabs, which is not a result of damage localisation.

4.4 Reflections and future work

Since the backing layer is not designed to contribute to the strength/stiffness of the composite, but is only necessary in order to handle the fabric, one can image possible solutions to the problem presented above:

(i) optimise the fibre arrangement of the backing,

(ii) change the backing fibres to a more compliant material (e.g. polyester) to reduce the interfacial stresses and stiffness mismatch between the layers,

(iii) apply a soft and thin interleaf (tackifier) between the axial bundles and the backing (see e.g. Tsotsis [11], or Hillermeier & Seferis [12]),

(iv) develop new stitching patterns that can stabilise and support the fabric so backing can be avoided.

The postulated fatigue damage sequence needs further investigation in order to be generalised. Ongoing studies try to describe the fretting behaviour observed between the backing and the axial layers as well as a numerical investigation of the effect of fibre debonding initiated due to the fibre breaks. Hopefully, these results will give a better idea of the best way to optimise the fibre/fabric architecture of a unidirectional composite.

5 Conclusion

Tension fatigue damage propagation in unidirectional glass fibre reinforced polymers (GFRP's) is investigated experimentally. The failure modes observed are similar for the different fibre volume fractions (FVF's) examined, but there is a remarkable difference on the fatigue life-time and the damage propagation rate depending on the FVF. A damage scheme is presented, explaining the reasons for tension fatigue damage in an axially loaded GFRP with backing fibres. The experimentally observed stiffness loss is caused by an initial failure of the backing layer forming a stress concentration and a fretting/rubbing mechanism that gives rise to broken fibres in the axial load-carrying bundles. Upon further cyclic loading, these mechanisms produce fibre debonding near the ends of the broken fibres. Finally, damage is localised and leads to final failure. Ongoing studies investigate in further detail the observations made in the present work.

References

[1] Brøndsted P., Andersen S., Lilholt H. Fatigue performance of glass/polyester laminates and the monitoring of material degradation. *Mechanics of composite materials*, **32(1)**, pp. 21–29, (1996).

[2] Beaumont P.W.R., Dimant R., Shercliff H. Failure processes in composite materials: getting physical. *Journal of materials science*, **41(20)**, pp. 6526–6546, (2006).

[3] Nijssen R.P.L. Fatigue life prediction and strength degradation of wind turbine rotor blade composites. *Contractor Report SAND2006-7810P, Sandia National Laboratories, Albuquerque, NM*, (2006).

[4] Gamstedt E.K., Talreja R. Fatigue damage mechanisms in unidirectional carbon-fibre-reinforced plastics. *Journal of Materials Science*, **34(11)**, pp. 2535–2546, (1999)

[5] Garrett K., Bailey J. Multiple transverse fracture in 90 cross-ply laminates of a glass fibre-reinforced polyester. *Journal of Materials Science*, **12(1)**, pp. 157–168, (1977).

[6] Reifsnider K. Fatigue behavior of composite materials. *International Journal of Fracture*, **16(6)**, pp. 563–583, (1980).

[7] Wang A., Kishore N., Li C. Crack development in graphite–epoxy cross-ply laminates under uniaxial tension. *Composites Science and Technology*, **24(1)**, pp. 1–31, (1985).

[8] Lafarie-Frenot M., Henaff-Gardin C., Gamby D. Matrix cracking induced by cyclic ply stresses in composite laminates. *Composites science and technology*, **61(15)**, pp. 2327–2336, (2001).

[9] Mao H., Mahadevan S. Fatigue damage modelling of composite materials. *Composite Structures*, **58(4)**, pp. 405–410, (2002).

[10]   Zhang Z., Hartwig G. Relation of damping and fatigue damage of unidirectional fibre composites. *International journal of fatigue*, **24(7)**, pp. 713–718, (2002).

[11]   Tsotsis T.K. Interlayer toughening of composite materials. *Polymer Composites*, **30(1)**, pp. 70–86, (2009).

[12]   Hillermeier R., Seferis J. Interlayer toughening of resin transfer molding composites. *Composites Part A: Applied Science and Manufacturing*, **32(5)**, pp. 721–729, (2001).